

Continuous electron shuttling by sulfide oxidizing bacteria as a novel strategy to produce electric current

de Rink, Riëks; Lavender, Micaela; Liu, Dandan; Klok, Johannes B.M.; Sorokin, Dimitry Y.; ter Heijne, Annemiek ; Buisman, Cees J.M.

DOI

[10.1016/j.jhazmat.2021.127358](https://doi.org/10.1016/j.jhazmat.2021.127358)

Publication date

2022

Document Version

Final published version

Published in

Journal of Hazardous Materials

Citation (APA)

de Rink, R., Lavender, M., Liu, D., Klok, J. B. M., Sorokin, D. Y., ter Heijne, A., & Buisman, C. J. M. (2022). Continuous electron shuttling by sulfide oxidizing bacteria as a novel strategy to produce electric current. *Journal of Hazardous Materials*, 424, 1-19. Article 127358. <https://doi.org/10.1016/j.jhazmat.2021.127358>

Important note

To cite this publication, please use the final published version (if applicable).
Please check the document version above.

Copyright

Other than for strictly personal use, it is not permitted to download, forward or distribute the text or part of it, without the consent of the author(s) and/or copyright holder(s), unless the work is under an open content license such as Creative Commons.

Takedown policy

Please contact us and provide details if you believe this document breaches copyrights.
We will remove access to the work immediately and investigate your claim.



Continuous electron shuttling by sulfide oxidizing bacteria as a novel strategy to produce electric current

Rieks de Rink^{a,b}, Micaela B. Lavender^a, Dandan Liu^b, Johannes B.M. Klok^{a,b,c},
Dimitry Y. Sorokin^{d,e}, Annemiek ter Heijne^{a,*}, Cees J.N. Buisman^{a,c}

^a Environmental Technology, Wageningen University, P.O. Box 17, Wageningen, The Netherlands

^b Paqell B.V., Reactorweg 301, 3542 AD Utrecht, The Netherlands

^c Wetsus, European Centre of Excellence for Sustainable Water Technology, Oostergoweg 9, Leeuwarden, The Netherlands

^d Winogradsky Institute of Microbiology, Research Centre of Biotechnology RAS, Leninskii Prospect, 33/2, 119071 Moscow, Russia

^e Department of Biotechnology, Delft University of Technology, Van der Maasweg 9, 2629HZ Delft, The Netherlands

ARTICLE INFO

Editor: Dr. J He

Keywords:

Bioelectrochemistry

Sulfide removal

Bio-anode

Microbial electrochemical system

Sulfide oxidizing bacteria (SOB)

ABSTRACT

Sulfide oxidizing bacteria (SOB) are widely applied in industry to convert toxic H₂S into elemental sulfur. Haloalkaliphilic planktonic SOB can remove sulfide from solution under anaerobic conditions (SOB are 'charged'), and release electrons at an electrode (discharge of SOB). The effect of this electron shuttling on product formation and biomass growth is not known. Here, we study and demonstrate a continuous process in which SOB remove sulfide from solution in an anaerobic 'uptake chamber', and shuttle these electrons to the anode of an electrochemical cell, in the absence of dissolved sulfide. Two experiments over 31 and 41 days were performed. At a sulfide loading rate of 1.1 mmolS/day, electricity was produced continuously (3 A/m²) without dissolved sulfide in the anolyte. The main end product was sulfate (56% in experiment 1 and 78% in experiment 2), and 87% and 77% of the electrons in sulfide were recovered as electricity. It was found that the current density was dependent on the sulfide loading rate and not on the anode potential. Biological growth occurred, mainly at the anode as biofilm, in which the deltaproteobacterial genus *Desulfurivibrio* was dominating. Our results demonstrate a novel strategy to produce electricity from sulfide in an electrochemical system.

1. Introduction

Hydrogen sulfide (H₂S) is a toxic and corrosive compound which can be present in several types of gas streams, such as natural gas and biogas (Krayzelova et al., 2015; Wenhui et al., 2010). Combustion of H₂S leads to the formation of sulfur dioxide, causing acid rain (Burns et al., 2016). For sustainable control of sulfur emissions, a biotechnological gas desulfurization process has been developed, which recovers biologically formed elemental sulfur (S⁰) (Buisman et al., 1989; Janssen et al., 1995). This process has been applied on commercial scale since the early nineties (Janssen et al., 2009; Klok et al., 2017).

The process solution consists of a sodium carbonate/bicarbonate buffer of ~1 M Na⁺ and the pH varies from 7.5 to 9.5. Sulfide is oxidized to (predominantly) S⁰ by haloalkaliphilic sulfide-oxidizing bacteria (SOB), with O₂ as final electron acceptor. Several sustainable aspects of this process are: (i) operation under ambient pressure and temperature;

(ii) no requirement of toxic chemicals, and (iii) S⁰ can easily be harvested from the process solution for reuse, for example as fertilizer (Van Zessen et al., 2004). Besides S⁰, sulfate (SO₄²⁻) and thiosulfate (S₂O₃²⁻) are formed, which are unwanted because it requires the addition of NaOH and, as a consequence, the formation of a bleed stream (De Rink et al., 2019; Klok et al., 2012; Van Den Bosch et al., 2007). The formation of SO₄²⁻ and S₂O₃²⁻ is stimulated at elevated O₂ concentrations and therefore the O₂ is controlled at very low concentrations.

To make the process more sustainable, recent studies focused on the reduction of chemical consumption (De Rink et al., 2019; Kiragosyan et al., 2020; Van Den Bosch et al., 2007). Another important aspect of the sustainability of biological gas desulfurization is the energy consumption, which is the focus of this study. In the current process, most of the energy consumption is related to the aeration of the bioreactor for O₂ supply. In addition, the process solution has to be cooled due to the heat released by the exothermic oxidation of sulfide. Therefore, the enthalpy

* Corresponding author.

E-mail address: annemiek.terheijne@wur.nl (A. ter Heijne).

¹ Visiting address: Bornse Weiland 9, Building Axis z, building nr. 118, 6708 WG Wageningen, The Netherlands.

of the oxidation of sulfide is lost.

Recently, it has been found that the SOB taken from the biodesulfurization process are electroactive. These planktonic bacteria can use an electrode as final electron acceptor, instead of O_2 (ter Heijne et al., 2018). Furthermore, it was demonstrated that these SOB can remove dissolved sulfide from solution under anaerobic conditions (de Rink et al., 2020; De Rink et al., 2019; ter Heijne et al., 2018). If this principle can be applied in a continuous electrochemical process for the removal of sulfide, this would have several benefits: (i) no energy is required for aeration (O_2 supply), and (ii) electrons are harvested from sulfide oxidation, which can be used to recover energy (e.g. in the form of H_2 , which can be formed at the cathode). Bioelectrochemical sulfide removal has been studied extensively (Ni et al., 2019; Rabaey et al., 2006; Sun et al., 2009; Zhang et al., 2009). However, one of the major drawbacks is the deposition of sulfur on the anode when the anode is contacted with dissolved sulfide directly. This deposition occurs due to an electrochemical reaction and will eventually lead to electrode passivation (Ateya et al., 2003; Dutta et al., 2008; Vaiopoulou et al., 2016). Thus, the challenge is to prevent direct contact between dissolved sulfide and the anode, which can be achieved by utilizing the shuttling capacity of SOB, as described by ter Heijne et al. (2018). This electron shuttling capacity of SOB is still poorly understood. In the batch experiments, the product formation and biomass growth could not be monitored (ter Heijne et al., 2018).

The aim of this study is to investigate a continuous bioelectrochemical process for the removal and conversion of sulfide using the sulfide shuttling capacity of SOB in the absence of O_2 . SOB are continuously circulated between a 'sulfide uptake reactor', to which sulfide is continuously added and where SOB can remove the dissolved sulfide from solution anaerobically, and the anode of an electrochemical cell, where electrons are released in the absence of dissolved sulfide. By shuttling SOB between this sulfide uptake reactor and the electrochemical cell, the sulfide removal and release of electrons is spatially separated. Furthermore, biomass growth and composition are studied to understand the underlying mechanisms of the overall process.

2. Materials and methods

2.1. Experimental set-up

Experiments were performed in a system consisting of an electrochemical cell, a sulfide uptake reactor (connected to the anode side of the electrochemical cell) and a catholyte recirculation reactor (connected to the cathode side), see Fig. 1. The liquid volume of the sulfide uptake reactor and catholyte recirculation reactor were 400 mL each. The working electrode (anode) was a graphite plate and the counter electrode a titanium plate coated with Pt/Ir O_2 (Magneto, special anodes, Schiedam, the Netherlands), both with an effective surface area of 22 cm 2 . A cation exchange membrane (FumaTech GmbH, Germany) was used to separate anode and cathode compartments, both with a volume of 33 mL. The anode compartment was filled with graphite granules (approximately 27 g) with a size of 2–4 mm (enViro-gran typ 514, enViro-cell, Oberursel, Germany) and the cathode compartment was filled with approximately 100 glass beads of 6–7 mm. An Ag/AgCl, 3 M KCl reference electrode (ProSense/QIS, the Netherlands) was connected to the anode chamber via a capillary. A potentiostat (nStat, multi-channel, Ivium, Eindhoven, the Netherlands) was used to control the anode potential and record the current.

First, the anode and cathode, including the recirculation reactors, were filled with an $NaHCO_3$ solution of approximately 1 M and liquid circulation was started. 1 M is a typical Na^+ concentration of the (full-scale) biodesulfurization process. To ensure anaerobic conditions in the system, the headspaces of recirculation reactors were continuously purged with a N_2/CO_2 gas stream of 4 L/h, dosed via Mass Flow controllers (Brooks). The pH was controlled by adjusting the ratio between the N_2 and CO_2 flow rates, which was approximately 4:1. After the O_2 concentration was below the detection limit (15 ppb), SOB biomass from an operating biodesulfurization installation was added to the sulfide uptake reactor. This installation is described by de Rink et al. (De Rink et al., 2019) and operated under similar conditions when the SOB were harvested. Approximately 10 mL inoculum was prepared by washing the

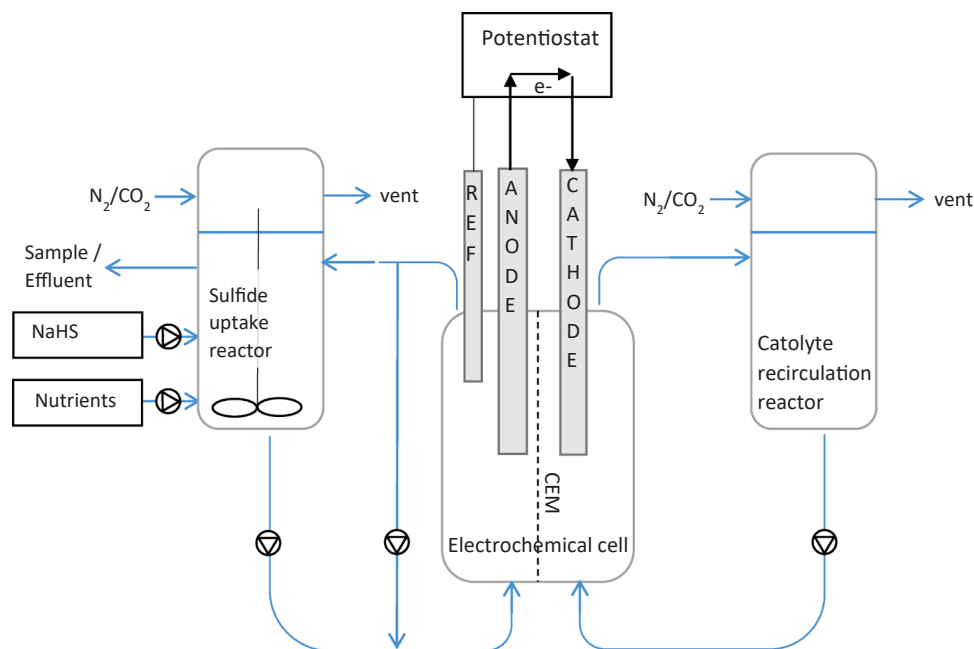


Fig. 1. Schematic drawing of experimental set-up. Sulfide was continuously added to the sulfide uptake reactor where SOB removed the sulfide from solution. The solution was circulated over the anode side of the electrochemical cell, where electricity was produced.

biomass to remove sulfur particles and (thio)sulfate. The biomass was centrifuged at 10,000 rcf and the biomass pellet was resuspended in 1 M NaHCO₃ solution. These steps were repeated 2 times.

Due to the anolyte liquid circulation, the planktonic SOB were continuously transferred from the sulfide uptake reactor to the anode side of the electrochemical cell and back. After about 1 h of liquid circulation, the dosing of NaHS and nutrients was initiated and the potentiostat was started. Gas bags filled with N₂ gas were connected to the headspaces of the NaHS and nutrient stock bottles in order to keep these anaerobic. NaHS was prepared by dissolving NaHS·xH₂O (hydro-sulfide hydrate pure flakes, Acros Organics) in demineralized water, which was extensively flushed with N₂. The sulfide concentration was verified by potentiometric titration with 0.1 M AgNO₃ using a TitrimoPlus titrator (Metrohm).

2.2. Operation of the continuous set-up

Two biotic (experiments 1 and 2) and one abiotic (experiment 3) were performed. In each experiment, the anode potential was changed stepwise and each potential was maintained for at least 4 days. All anode potentials are reported versus Ag/AgCl, 3 M KCl.

2.2.1. Experiment 1

Experiment 1 had a total duration of 31 days and the applied anode potentials were -0.1, -0.2, -0.3, -0.35 and -0.4 V. The NaHS concentration in the stock solution was 20.45 gS/L and was continuously dosed into the sulfide uptake reactor with a flow rate of 1.66 g/day, resulting in a constant sulfide loading rate of 1.06 mmolS/day. The circulation flow rate over the sulfide uptake reactor was 0.6 L/h, which resulted in an HRT of 40 min in the sulfide uptake reactor. Nutrients solution consisted of macro nutrient as described by de Rink et al. (De Rink et al., 2019) and 1 mL/L trace element mix as described by Pfennig and Lippert (1966). The nutrient dosing rate was set in such way that the total residual nitrogen concentration in the supernatant was <10 mgN/L. In this way, overdosing of nutrients is prevented and the bacteria consume all nutrients. This dosing strategy is similar to full-scale biodesulfurization installations.

H₂ cross-over from cathode to anode could influence the current production. To rule out effects of H₂ cross-over, on day 15 of experiment 1, [Fe(CN)₆]³⁻ was added to the catholyte recirculation reactor. After addition of [Fe(CN)₆]³⁻, the cathode potential changed, but the current did not change, indicating that H₂ cross-over did not influence the anodic oxidation reaction, and thus the current, in the electrochemical cell. However, from day 16 onwards, it was noticed that total and dissolved N concentrations increased, even after nutrient dosing was stopped at day 21. Probably some [Fe(CN)₆]³⁻ leaked through the membrane into the anode compartment. From day 16 onwards, the difference between total-N and dissolved-N concentrations still represents the concentration of planktonic bacteria, but an accurate N-balance, including calculation of the amount of biofilm, could not be made.

2.2.2. Experiment 2

Experiment 2 had a total duration of 41 days and the applied anode potentials were -0.1, -0.2, -0.3, and -0.4 V. The NaHS concentration in the stock solution was lowered to 8.90 gS/L in order to have a higher inflow rate. Furthermore, the nutrients were diluted 2x and the dosing rate was doubled compared to experiment 1. The sulfide loading rate in experiment 2 varied in order to find the maximal sulfide uptake capacity of the bacteria. Initial loading rate was 0.79 mmolS/day. From day 12–29, the loading rate was increased to 1.16 mmolS/day; from day 30–42, the sulfide loading rate was again 0.79 mmolS/day. The

recirculation flow rate over the anolyte recirculation vessel was decreased to 0.42 L/h, resulting in an HRT of 58 min.

2.2.3. Experiment 3

Experiment 3 was an abiotic experiment, performed after experiment 2. Despite thorough cleaning of the system and replacement of the graphite granules, some biological activity was observed in this abiotic experiment. Therefore, approximately 0.1 M sodium azide (NaN₃) was added to the system, after which the system was considered abiotic. The effect of NaN₃ on the current production was verified with cyclic voltammetry in a separate electrochemical cell and no effect on the current was observed in the potential range of our experiments. The abiotic experiment was performed for 10 days and the applied anode potentials were -0.1 and -0.4 V. The sulfide loading rate was 0.99 mmolS/day and no nutrients were dosed. The liquid circulation rate in experiment 3 was also 0.42 L/h, corresponding to an HRT in the anolyte recirculation vessel of 58 min.

2.2.4. Other experimental conditions

An overview of the flow rates, volumes in the different parts of the system and the HRT's in the different parts of the system in each experiment is provided in the [Supplementary Material \(A\)](#). During all 3 experiments, the pH was controlled around 8.3 by adjusting the CO₂ flow rate to the headspaces of the recirculation reactors. The initial alkalinity (i.e. bicarbonate concentration) was 1.0 M and conductivity was 52 mS/cm. Due to acidification and dilution, the alkalinity and conductivity decreased during the experiments. For example, at the end of the experiment 1, the alkalinity and conductivity were 0.37 M and 31 mS/cm. Under the applied pH (~8.3), practically all sulfide is present as HS⁻. Based on the measured current and the product formation, the electron balance is reasonable, which confirms that release of gaseous H₂S is negligible.

The thermodynamics of any (bio)electrochemical system is determined by both anode and cathode reactions and their corresponding potentials. In our experiments, the cathode potential was approximately -0.8 V to form H₂. This consumed electricity, but energy is recovered in the form of hydrogen gas.

2.3. Analyses

Daily samples were taken from the sulfide uptake reactor. A sample from the catholyte recirculation reactor was taken at the end of the experiments. pH and conductivity were analyzed offline using a HQ440d multi analyzer (Hach, Germany). Alkalinity, expressed as [HCO₃⁻] was measured with an automated TitrimoPlus titrator (Metrohm) by titrating to pH 4.3 using a 0.1 M HCl solution. SO₄²⁻ and S₂O₃²⁻ concentrations were determined on the samples supernatant (after centrifuging for 10 min at 14,000 g) using a Dionex ICS-2100 Ion Chromatograph (ThermoScientific) with a Thermo Fisher Scientific IonPac AG17 Guard (Thermo Fisher Scientific, Waltham, MA, USA) and Thermo Fisher Scientific IonPac AS17 column (Thermo Fisher Scientific) at 30 °C. The eluent was KOH at a flowrate of 1.0 mL/min. The sample injection volume was 10 µL. The biomass concentration was measured as the amount of total organic N using the Dr. Lange cuvette test LCK138 (Hach Lange, Germany), as described by De Rink et al. (2019). The difference between the supernatant (i.e., a sample centrifuged for 10 min at 14,000 g) and a non-centrifuged sample indicated the total amount of N present in the (planktonic) biomass. To exclude interference by salts and biologically produced S⁰, the samples were diluted at least 5 times. Based on the amount of N added with the nutrients and the measured N concentrations, an N-balance was made in order to calculate the amount

of biomass attached to the electrode (biofilm), see Eq. (7). The dissolved sulfide concentration in the sulfide uptake reactor was measured using the Hach Lange cuvette test LCK635 (Hach Lange, Germany). Furthermore, lead acetate paper (Merck) was used to check presence/absence of dissolved sulfide. The O₂ concentration in the headspaces of the anode and cathode chambers was measured with oxygen sensor spots and Fibox 4 trace meter (PreSens, Regensburg Germany).

During each run, the experiment was occasionally interrupted to make polarization curves (determine current production at a range of anode potentials). The applied potentials were -0.5, -0.45, -0.4, -0.35, -0.3, -0.2 and -0.1 V (vs Ag/AgCl) and current was measured each second. Each potential was maintained for 5 min and the last measurement for each potential was taken as the current production at the respective anode potential. During the polarization curves, the sulfide dosing was maintained. The microbial communities of the planktonic bacteria and biofilm were analyzed using 16S amplicon sequencing. Samples were taken from the liquid and the graphite granules at the end of each run. Also a sample of the inoculum (planktonic biomass) was analyzed. Details of the analysis can be found in the

$$P_{S_8-S} = I_{HS^-} - P_{SO_4^{2-}-S} - P_{S_2O_3^{2-}-S} \quad (3)$$

Here, P_{S_8-S} , $P_{SO_4^{2-}-S}$ and $P_{S_2O_3^{2-}-S}$ are the productions of S⁰, SO₄²⁻, and S₂O₃²⁻, respectively, in mol S-product and I_{HS^-} is the volumetric HS⁻ influent in mol S. Overall product selectivities were:

$$\text{Overall } S_{SO_4^{2-}-S} (\%) = \frac{\text{Total } P_{SO_4^{2-}-S} (\text{mol S})}{\text{Total } I_{HS^-} (\text{mol S})} \quad (4)$$

$$\text{Overall } S_{S_2O_3^{2-}-S} (\%) = \frac{\text{Total } P_{S_2O_3^{2-}-S} (\text{mol S})}{\text{Total } I_{HS^-} (\text{mol S})} \quad (5)$$

$$\text{Overall } S_{S_8-S} (\%) = \frac{\text{Total } P_{S_8-S} (\text{mol S})}{\text{Total } I_{HS^-} (\text{mol S})} \quad (6)$$

The amount of biofilm, expresses as mg-N per liter of the total system volume was calculated as the difference between the measured total-N concentration and the theoretical total-N concentration. The theoretical total-N concentration ($N_{\text{theor.}}$) was calculated according to Eq. (7):

$$N_{\text{theor. day } x} \left(\frac{\text{mgN}}{\text{L}} \right) = N_{\text{theor. day } x-1} + \left(\frac{N \text{ added with nutrients} - (\text{measured total} - N\text{-Effluent})}{V} \right) \quad (7)$$

Supplementary Material (B). The EMBL-EBI accession number for the presented 16S rRNA sequencing set is PRJEB44164.

At the end of the experiments, presence of elemental sulfur on the electrode was verified using XRD analysis. Details can be found in the **Supplementary Material (C)**.

2.4. Calculations

The production of SO₄²⁻-S (Eq. 1) and S₂O₃²⁻-S (Eq. 2) were calculated as follows:

$$P_{SO_4^{2-}-S} = \text{effluent} \cdot [\overline{SO_4^{2-}-S}] + V \cdot \Delta [SO_4^{2-}-S] \quad (1)$$

$$P_{S_2O_3^{2-}-S} = \text{effluent} \cdot [\overline{S_2O_3^{2-}-S}] + V \cdot \Delta [S_2O_3^{2-}-S] \quad (2)$$

Here, *effluent* is the effluent of the system (i.e. the sample volume from the sulfide uptake reactor) (L), $[\overline{SO_4^{2-}-S}]$ and $[\overline{S_2O_3^{2-}-S}]$ are the average concentrations (mol-S L⁻¹) of two consecutive samples, V is the total liquid volume of the system and $\Delta [SO_4^{2-}-S]$ and $\Delta [S_2O_3^{2-}-S]$ are

In Eq. (7), *N added with nutrients* is calculated as the total-N concentration in the nutrients \times the amount of dosed nutrients between day_{x-1} and day_x. *Effluent* is the amount of effluent between day_{x-1} and day_x.

Based on the formed products, the total amount of released electrons was calculated. The amount of e⁻ released per S⁰ formed, is 2 (Eq. 8); for each mol of SO₄²⁻ produced, an additional amount of 6 mol e⁻ is released, i.e. a total of 8 mol e⁻ (Eq. 9).



The amount of electrons harvested at the anode was determined based sum of the current (as logged by the potentiostat). Based on the SO₄²⁻ formation, the amount of e⁻ used for biomass growth was calculated based on the work of Klok et al. (2012). Based on this electron balance, the coulombic efficiency (CE) was calculated excluding biomass growth (Eq. 10) and including biomass growth (Eq. 11).

$$CE_{\text{excl biomass}} (\%) = \frac{e^- \text{ harvested at anode}}{e^- \text{ released by } S^0 \text{ production} + e^- \text{ released by } SO_4^{2-} \text{ production}} \quad (10)$$

$$CE_{\text{incl biomass}} (\%) = \frac{e^- \text{ harvested at anode} + e^- \text{ to biomass growth}}{e^- \text{ released by } S^0 \text{ production} + e^- \text{ released by } SO_4^{2-} \text{ production}} \quad (11)$$

the concentration changes (mol-S L⁻¹) between the samples. At the end of the experiments, some SO₄²⁻ was detected in the catholyte (<5% of the concentration in the anolyte). Hence this was not taken into account in the calculation for the SO₄²⁻ production.

As no products other than S₈, SO₄²⁻ and S₂O₃²⁻ were measured in the reactor, and it was not possible to quantify the amount of S₈ (Van Den Bosch et al., 2007), production of S₈ was calculated from the mass balance:

3. Results and discussion

Two experiments were performed, in which planktonic bacteria continuously removed the supplied sulfide from solution in the sulfide uptake reactor and subsequently released electrons at the anode of the (bio)electrochemical cell. The results of these two experiments are

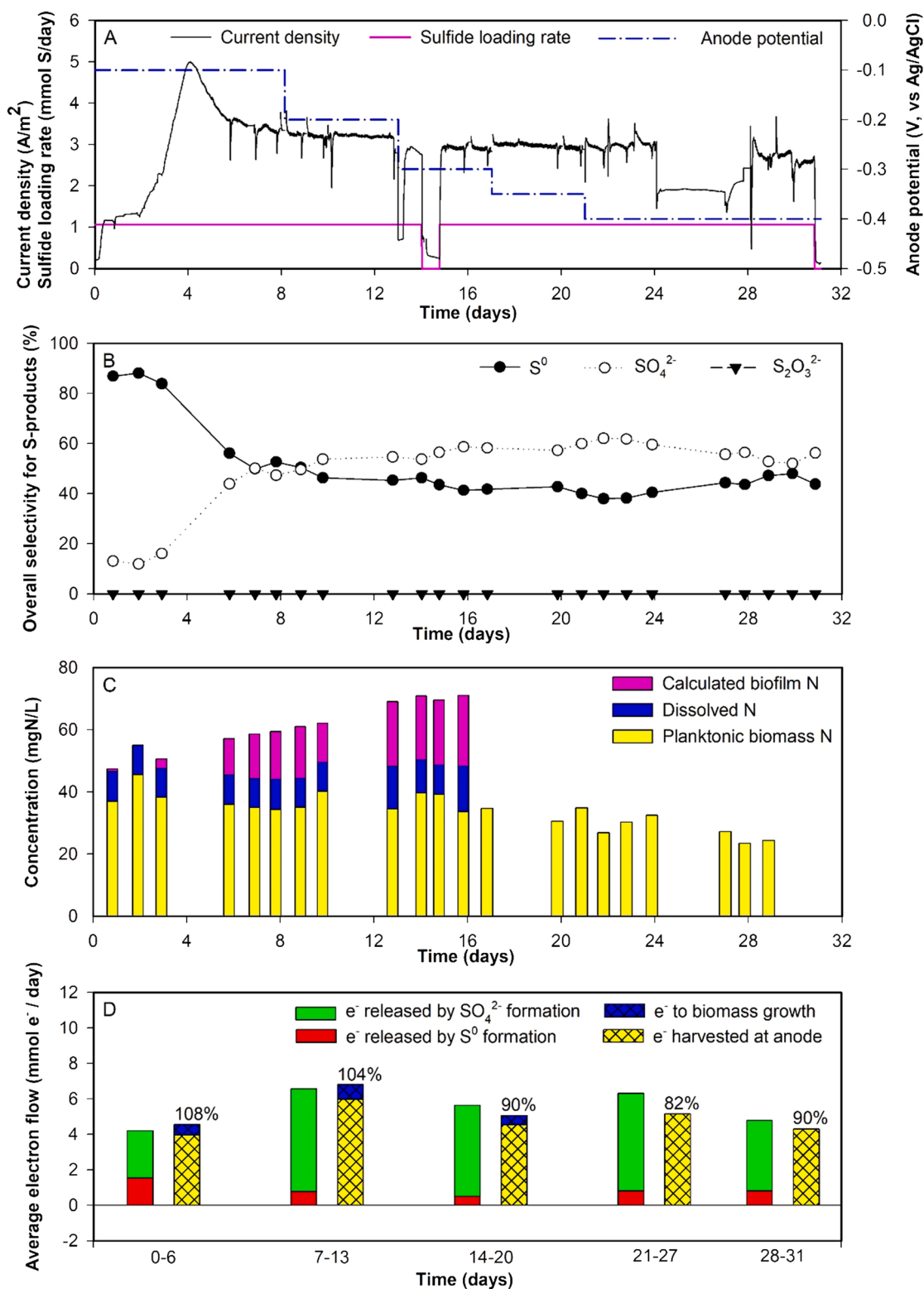


Fig. 2. Results of experiment 1. A shows the sulfide dosing rate, applied anode potential and current production; in Fig. B the overall selectivities for the S-products is shown; C shows the measured planktonic biomass concentration and the calculated concentration of biofilm (based on the total system's volume); in D the electron balance is shown.

shown in Fig. 2 (experiment 1) and 3 (experiment 2), and the performance of the reactors will be described and discussed in the following chapters.

3.1. Continuous electric current production in absence of dissolved sulfide

Figs. 2A and 3A show the sulfide loading rate, the applied anode potential and the resulting current density. In both experiments, current density increased during the first days of the experiment and reached a

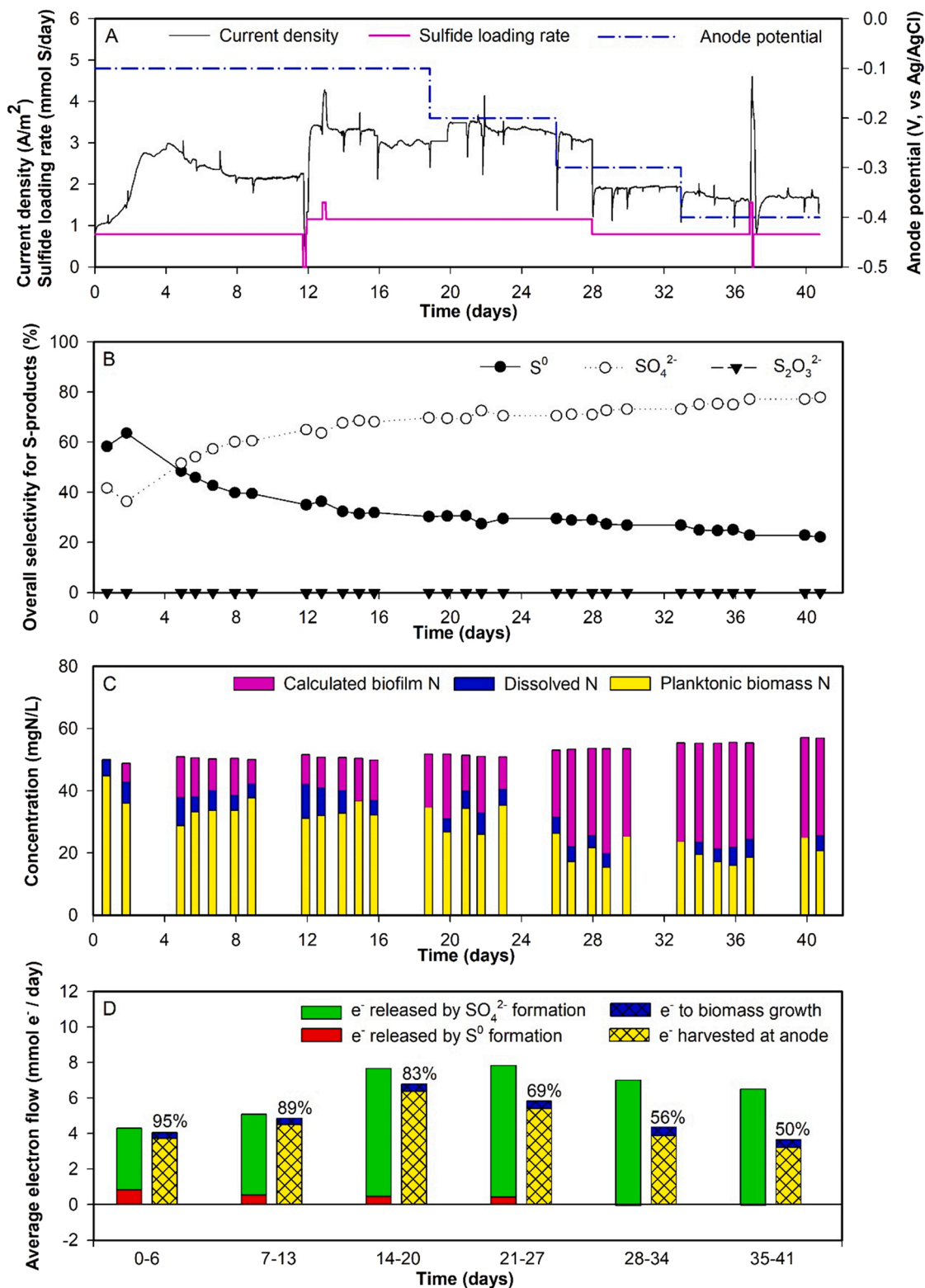


Fig. 3. Results of experiment 2. A shows the sulfide dosing rate, applied anode potential and current production; in Fig. B the overall selectivities for the S-products is shown; C shows the measured planktonic biomass concentration and the calculated concentration of biofilm (based on the total system's volume); in D the electron balance is shown.

peak at day 5. Thereafter, current decreased and stabilized.

In experiment 1, the sulfide load was constant at 1.06 mmol/day (see Fig. 2A). Throughout the experiment, all supplied sulfide was converted. In the first 3 days, the current density was approximately 1 A/m². In this period, sulfide was converted into predominantly S⁰ (see Fig. 2B). After

the third day, the current density increased and eventually stabilized around 3 A/m² at day 6. On day 3–6, the selectivity for SO₄²⁻ increased and consequently, the selectivity for S⁰ decreased. Since SO₄²⁻ formation releases more electrons than S⁰ formation, the increase in the current density was related to the increase in SO₄²⁻ formation. The product

formation is discussed in more detail in Section 3.2. The theoretical dissolved sulfide concentration in the sulfide uptake reactor was 0.07 mM, based on sulfide loading and recirculation flow rate. However, no dissolved sulfide was detected in the anolyte during the entire run, except for days 3 and 14 where some dissolved sulfide was detected (see Supplementary Material D). Thus, sulfide was removed by SOB in the sulfide uptake reactor, and the average sulfide uptake was 2.06 $\mu\text{mol}/\text{mgN}$, based on an average biomass concentration of 34 mgN/L . At day 14, an unstable current was measured, and dissolved sulfide was detected in the anolyte. Therefore, the sulfide dosing was stopped overnight and the cable connections between the potentiostat and the three electrodes were verified. The following day, the sulfide dosing was restarted and no more dissolved sulfide was detected in the anolyte. In addition, the current density stabilized at previously obtained value of 3 A/m^2 . From day 24–27 the measured current density was lower, due to an offset of the reference electrode. After replacement of the reference electrode, the measured current density returned to 3 A/m^2 . In this period, sulfide uptake in the sulfide uptake reactor continued, and no dissolved sulfide was detected in the sulfide uptake reactor.

Also throughout experiment 2, all supplied sulfide was converted. Experiment 2 was started with a sulfide loading rate of 0.79 mmolS/day . The initial current density was 1 A/m^2 , which stabilized around 2 A/m^2 at day 8 (see Fig. 3A). In the first days of experiment 2, the same pattern as in experiment 1 was observed: Initially, the selectivity for S^0 formation was high. When SO_4^{2-} formation increased, the current density became higher. No dissolved sulfide was detected in the sulfide uptake reactor until day 12. Therefore, at day 13 the sulfide load was increased to 1.16 mmolS/day , which resulted in an increase in the current density, and still no dissolved sulfide was detected in the anolyte. Hence, the sulfide uptake was 3.5 $\mu\text{mol}/\text{mgN}$ during this period, which was 32% higher than in experiment 1. After a second increase to 1.56 mmolS/day , the current density reached a value of 3.84 A/m^2 . However, after the second increase, dissolved sulfide was detected with lead acetate paper (not quantified) and the sulfide load was reduced to 1.16 mmolS/day . At this dosing rate, the measured current density was around 3 A/m^2 , similar to the current density measured in experiment 1. From day 20 onwards, detectable quantities of dissolved sulfide were present in the anolyte. However, the majority of sulfide was still being removed (Supplementary Material D). At day 28, the sulfide loading rate was decreased to the initial value of 0.79 mmolS/day , resulting in a current of 1.8 A/m^2 .

In both runs, the initial applied anode potential was -0.1 V vs Ag/AgCl . From previous batch experiments, this anode potential was found to be sufficiently high to recover electrons from ‘charged’ SOB (ter Heijne et al., 2018). During the experiment, polarization curves were recorded (results discussed in Section 3.5). From these curves, it appears that current production is possible at anode potentials $<-0.1\text{ V}$ vs Ag/AgCl . Theoretically, a lower anode potential results in a lower driving force for electron transfer. When the driving force is too low, no current can be generated. To study the effect of anode potential, the applied anode potential was stepwise decreased to -0.4 V in both experiments. Surprisingly, this decrease did not have an effect on the current density. In our experiments, decreasing the anode potential from -0.1 V to -0.4 V did not result in an increase in the selectivity for S^0 formation. Since the current density at constant sulfide loading rate is dependent on the product formation (i.e. S^0 and SO_4^{2-}), the current density did not change when the anode potential was changed. The current density did change when the sulfide loading rate was changed (in experiment 2). Thus, in addition to the product selectivity, also the substrate supply determined the measured current density.

3.2. Product formation

Figs. 2B and 3B show the overall product selectivities in experiments 1 and 2. In both experiments, no thiosulfate ($\text{S}_2\text{O}_3^{2-}$) was detected. While $\text{S}_2\text{O}_3^{2-}$ is a reaction product of chemical oxidation of dissolved sulfide

with oxygen (O’Brien and Birkner, 1977; Van den Bosch et al., 2008), its absence can be explained by the absence of dissolved sulfide and/or the absence of O_2 in the anolyte. At the start of both experiments, the selectivity for S^0 formation was higher than for SO_4^{2-} formation. However, after a few days of operation, SO_4^{2-} rather than S^0 became the main end product of sulfide oxidation. Bacteria prefer SO_4^{2-} formation over S^0 formation due to the higher Gibbs free energy. In the conventional biological desulfurization process, SO_4^{2-} formation is minimized by limiting the O_2 supply (Klok et al., 2012; Van Den Bosch et al., 2007). The product formation also depends on the microbial community, which is discussed in Section 3.6. In this section, the mechanisms of SO_4^{2-} formation are further discussed.

For experiment 1, the overall selectivity for SO_4^{2-} formation was 56% and the selectivity for S^0 formation 44%. For experiment 2, the selectivity for SO_4^{2-} was 78% and selectivity for S^0 22%. From day 28 onwards, all HS^- dosed was converted into SO_4^{2-} . In none of the experiments, S_8 -sulfur was detected on the granules or graphite plate, as confirmed with XRD analysis. Occasional analysis of the total sulfur concentration in the anolyte with inductively coupled plasma optical emission spectrometry showed that the total sulfur concentration was higher than the sum of the $\text{SO}_4^{2-}\text{-S}$ and $\text{S}_2\text{O}_3^{2-}\text{-S}$ concentration as analyzed with ion chromatography, indicating that also elemental sulfur was present in the anolyte. The overall obtained selectivities for S^0 formation are similar to the results of Ni et al. (Ni et al., 2019) who obtained a selectivity for S^0 formation of 40% in a fed-batch reactor set-up with a similar electrochemical cell. In the conventional biological desulfurization process a selectivity for sulfur formation of 97% has been achieved (De Rink et al., 2019).

3.3. Biomass growth

The amount of biomass in the system is shown in Fig. 2C (experiment 1) and 3C (experiment 2). The yellow bars represent the biomass of planktonic cells. The blue bars show the measured dissolved N concentration, which is most likely resulting from non-consumed nutrients in the form of urea and/or ammonium. The concentration of planktonic biomass slightly decreased over the course of both experiments (i.e. the yellow bars in Figs. 2C and 3C). This means that the loss of planktonic bacteria via the effluent is higher than the increase of planktonic bacteria via bacterial growth. Based on the nutrient dosing rate, a higher total nitrogen concentration in the effluent was expected. For example, at the end of run 2, the measured biomass was about 50% lower than expected based on the supply of nutrients. Thus, there is another nitrogen sink, which is most likely the formation of a biofilm on the anode. The amount of biofilm could be calculated based on the addition of nutrients and the measurement of the nitrogen concentration in the anolyte. This amount, expressed as mgN/L of the total system, is represented by the purple bars in the Figs. 2C and 3C. Hence, the height of the bars represents the total amount of N in the system, which consist of biofilm, planktonic bacteria and non-consumed nutrients.

From Figs. 2C and 3C it appears that growth of sulfur metabolizing bacteria occurred, i.e. the bulk of the dosed nutrients were consumed. The majority of the growth occurred at the anode in the form of biofilm. At the end of experiment 2, the amount of biofilm-N on the electrode was determined by measuring the total N concentration of the granules, and was found to be 10.85 mgN . This translates to 31.46 mgN/L based on the total volume of the system and is in agreement with the amount of biofilm calculated based on the N-balance (31.28 mgN/L).

3.4. Electron balance

Based on the average values for produced current, product formation and biomass growth, electron balances were made for periods of a week of operation. Results are shown in Figs. 2D and 3D.

For experiment 1 (Fig. 2D), during day 0–6, the average rate of electrons released was 4.2 $\text{mmol e}^-/\text{day}$, of which 37% was coming from

oxidation of HS^- to S^0 and 63% from the oxidation of HS^- to SO_4^{2-} . In this period, the rate of harvesting electrons at the anode was $4.0 \text{ mmol e}^-/\text{day}$, which was 94% of the e^- released from HS^- . When taking into account the calculated e^- used for biomass growth ($0.16 \text{ mmol e}^-/\text{day}$), the coulombic efficiency was 108%. The coulombic efficiencies varied over the time periods. The overall coulombic efficiency during experiment 1 was 87%.

During experiment 2, the coulombic efficiencies were around 90% (up to day 20). Towards the end of the experiment the coulombic efficiency decreased for unknown reasons and was 56% in the period of day 35–41. In this period it was noticed that the formation of SO_4^{2-} was slightly higher than the amount of HS^- supplied. This can be explained by SO_4^{2-} production from S^0 which has been formed in the initial stage of the experiment. As a result, from day 28–41, the net production of S^0 formation is negative. Hence, the e^- released by S^0 formation (the red bar in Fig. 3D) in this period is expressed as a negative number. The overall coulombic efficiency during experiment 2 was 77%. The coulombic efficiencies obtained in the experiments are higher than reported by Ni et al. (48.4%), who used a similar medium, but higher sulfide concentrations (Ni et al., 2019).

3.5. Biotic vs abiotic operation

To study the effect of the presence of SOB on HS^- removal, an abiotic control experiment was performed at anode potentials of -0.1 V and -0.4 V . In this experiment, sodium azide (NaN_3) was added to the system. Azide is a general agent to block growth of aerobic bacteria by the inhibition of the terminal cytochrome c oxidases of their respiratory chain (Lichstein and Soule, 1944; Solioz et al., 1982). Addition of NaN_3 had a direct effect on the current density. After each addition, the current density dropped. After the first addition (1.7 g/L), the current density dropped, but started to increase after several hours. Therefore, more NaN_3 was added (total 6.8 g/L) until no direct effect on current density was observed anymore; at this moment the current was almost zero. After the 4th addition, the experiment was considered abiotic. It was confirmed in a separate batch test that azide did not react with the electrode under the applied process conditions.

Under the abiotic conditions, dissolved sulfide was present in the sulfide uptake reactor at all times. For the abiotic experiment the system was operated at an anode potential of -0.1 V for 4 days. During this period, a current density of 0.46 A/m^2 was obtained at a sulfide dosing

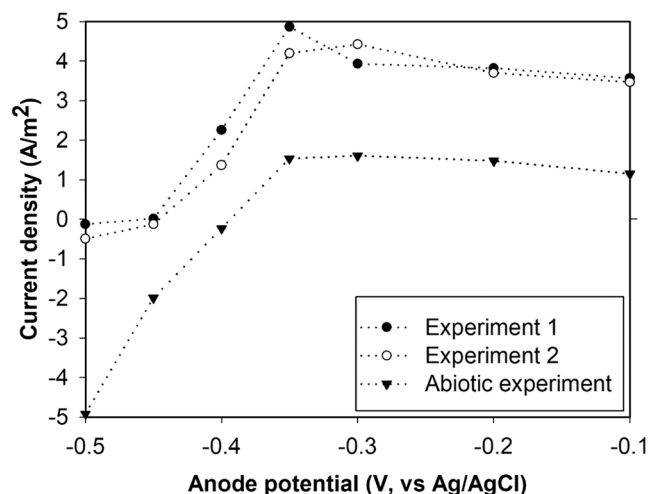


Fig. 4. Typical polarization curves for the biological runs 1 and 2 and the abiotic control experiment. Polarization curves were made by stepwise increasing the anode potential (from -0.5 to -0.1 V) and measuring the current. Each potential was maintained for 5 min to obtain a stable current at the applied potential. The plotted values are the last measured value.

rate of 0.99 mmolS/day . This is considerably lower than the 3 A/m^2 that was measured in the presence of bacteria. At the same time, sulfide levels increased in the anolyte during the abiotic experiment, indicating that sulfide uptake in the sulfide uptake reactor only occurred with planktonic bacteria. Both SO_4^{2-} and $\text{S}_2\text{O}_3^{2-}$ were produced at rates of 0.14 mmol/day and 0.08 mmolS/day . Interestingly, $\text{S}_2\text{O}_3^{2-}$ was not detected in the biotic experiments because no dissolved sulfide was present. At an anode potential of -0.4 V , the current density was negative (-0.1 A/m^2). This means that electrons flowed in reverse direction, i.e. from counter electrode to working electrode. Biotic and abiotic polarization curves are shown in Fig. 4. For the biotic experiments, a slightly negative current was observed at anode potentials of -0.5 and -0.45 V . For higher anode potentials, current density was positive. Under abiotic conditions, the current density was still negative at an anode potential of -0.4 V and positive at potentials of -0.35 V and higher. A further increase in anode potential did not result in higher current density. Between -0.35 and -0.1 V the anode potential did not influence the current. Under these conditions, the current density was determined by sulfide dosing and not by the anode potential.

3.6. Microbial community

The microbial community of the planktonic bacteria and the biofilm was analyzed at the end of each run. The inoculum, obtained from a pilot-scale biodesulfurization plant, was also analyzed. Results are shown in Table 1. The inoculum contains *Thioalkalivibrio* (relative abundance 32%) and *Alkalilimnicola* (18%). Both are haloalkaliphilic SOB. *Thioalkalivibrio sulfidophilus* has previously been found to be the dominant SOB in both full-scale and lab scale biodesulfurization installations (Sorokin et al., 2012, 2008b). Genome analysis indicates that it oxidizes HS^- to S^0 via flavocytochrome c (Fcc) sulfide dehydrogenase and S^0 to SO_4^{2-} via the reversed DSR pathway (Muyzer et al., 2011). *Alkalilimnicola* species are facultatively autotrophic and facultatively anaerobic SOB (Hoeft et al., 2007; Sorokin et al., 2006). It has been suggested that some *Alkalilimnicola* members are limited to partial sulfide oxidation to S^0 (De Rink et al., 2019).

At the end of each experiment, the microbial community of both the planktonic and the biofilm biomass had undergone considerable changes. In both experiments, the biofilm was dominated by bacteria belonging to the genus of *Desulfurivibrio*, with a relative abundance of 37.0% in experiment 1% and 43.3% in experiment 2. *Desulfurivibrio* is also present in the planktonic biomass (21.6% and 11.1%), while the relative abundance of *Desulfurivibrio* in the inoculum was only 1.3%. The genus includes a single species: *Desulfurivibrio alkaliphilus* (Sorokin and Merkel, 2020). Until now, *Desulfurivibrio alkaliphilus* was only found in soda lakes (Sorokin et al., 2020, 2008a). It is an obligately anaerobic deltaproteobacterium originally described as sulfur-thiosulfate reducer. However, more recently it was found that *Desulfurivibrio alkaliphilus* is a chemolithoautotrophic sulfur disproportionator (Poser et al., 2013). This means it is using S^0 as both electron acceptor and donor, dismutating it to 1 mol SO_4^{2-} and 3 mol HS^- . Furthermore, it can also couple the oxidation of sulfide to sulfate to the reduction of nitrate/nitrite to ammonium (Müller et al., 2016; Thorup et al., 2017). In our experiments, the N-source was urea and NO_3^{2-} and NO_2^{2-} were not supplied. Therefore, *Desulfurivibrio alkaliphilus* could have been responsible for the formation of SO_4^{2-} , but it is not clear whether it was contributing to the observed bioelectrochemical HS^- oxidation to elemental sulfur. *Desulfurivibrio alkaliphilus* is related to the long-distance electron transferring cable bacteria (Müller et al., 2016; Thorup et al., 2017). Furthermore, it possess genes for the expression of conductive pili, which are used for external electron transfer (Walker et al., 2018). The dominance of *Desulfurivibrio alkaliphilus* in the biofilm was also observed by Ni et al. (2019).

It must be noted that electricity was produced immediately from the start of the experiment, i.e. with only planktonic bacteria. Since the relative abundance of *Desulfurivibrio* in the inoculum was only 1.28%,

Table 1

Overview of the key bacterial species in the solution (planktonic biomass) and attached to the electrode (biofilm) as analyzed via 16 S rRNA amplicon sequencing. An extensive table of the present species is provided in the [Supplementary Material B](#).

	Relative abundances					Key physiology	Occurrence
	Inoculum	End of exp 1 (planktonic)	End of exp 1 (biofilm)	End of exp 2 (planktonic)	End of exp 2 (biofilm)		
Sulfide oxidizing bacteria (SOB)							
<i>Alkalilimnicola</i>	18.48%	18.58%	4.02%	6.36%	1.94%	facultatively autotrophic and facultatively denitrifying SOB	Soda lakes and biodesulfurization plants
<i>Thioalkalispirilla</i>	0.22%	1.21%	0.12%	3.34%	0.23%	microaerophilic lithoautotrophic SOB	Soda lakes
<i>Thioalkalivibrio</i>	31.88%	2.54%	0.75%	16.40%	9.93%	Lithoautotrophic SOB	Soda lakes and Thiopaq reactors
<i>Thioalkalimicrobium</i>	3.00%	2.90%	0.34%	0.73%	0.99%	Lithoautotrophic SOB	Soda lakes and Thiopaq reactors
<i>Rhodobacteraceae / other</i>	28.75%	2.59%	0.42%	9.38%	2.43%	Might be photoheterotrophic anaerobic SOB	Might be in soda lakes
<i>Arcobacter</i>	0.06%	3.08%	0.08%	14.30%	0.86%	Microaerophilic sulfide oxidation	Marine
Anaerobic sulfur bacteria							
<i>Desulfurivibrio</i>	1.28%	21.59%	36.97%	11.11%	43.31%	Elemental sulfur disproportionation or sulfur reduction with H ₂	Biodesulfurization plants
<i>Desulfurispirillum</i>	0.35%	1.10%	6.03%	0.35%	1.38%	Sulfur reduction; dissimilatory ammonification	Soda lakes
Fermentative bacteria							
<i>Acholeplasma</i>	0.58%	6.10%	0.67%	3.44%	1.99%	Fermentative	Found in soda lake metagenomes
<i>Anoxynatronum</i>	0.83%	0.92%	1.30%	0.28%	2.73%	Fermentative	Soda lakes
<i>Tindallia</i>	0.40%	0.14%	1.89%	0.16%	1.51%	Acetogenic, can use H ₂ and reduce thiosulfate	Soda lakes
Uncultured (<i>cloacimonetes</i>)	0.00%	2.12%	2.84%	0.10%	0.40%	Fermentative	Found in soda lake metagenomes
Hydrolytic bacteria							
<i>Lentimicrobiaceae / uncultured</i>	0.24%	15.69%	3.69%	16.13%	8.02%	Polysaccharidolytic	Soda lakes
<i>Natronoflexus</i>	0.00%	0.03%	7.31%	0.01%	0.45%	sugar fermentation	Soda lakes

Desulfurivibrio is not the only species that can exchange electrons with the electrode and that a biofilm is not required for the electricity production. This is in agreement with the experiments of [ter Heijne et al. \(2018\)](#), in which no biofilm was present.

At the end of run 1, the relative abundance of *Alkalilimnicola* in the solution was still 18%, while the relative abundance of *Thioalkalivibrio* decreased to 2.5%. In run 2, relative abundances of both *Alkalilimnicola* (6%) and *Thioalkalivibrio* (10%) in the solution had decreased.

3.7. Considerations

In this paper we demonstrated a continuous electrochemical process to simultaneously remove sulfide, produce elemental sulfur and recover energy. In this process, the removal of sulfide and release of electrons was spatially separated by applying the electron shuttling capacity of SOB. Our results show that continuous release of electrons by SOB took place in absence of dissolved sulfide at the anode. Furthermore, it was shown that biomass growth occurred.

However, there is still room for improvement, e.g. with respect to product formation. In both experiments, the main product was sulfate. Sulfate formation is unwanted, because it requires NaOH addition to prevent acidification of the process solution. In experiment 1, the overall selectivity for sulfur formation was 44% and in experiment 2, the selectivity for sulfur formation was 22%.

Even though the aim was to grow planktonic biomass, which can be recirculated between sulfide uptake reactor and the anode compartment, it was found that biomass was accumulating on the electrode, while the amount of planktonic biomass slightly decreased during the experiments. This suggests that most of the metabolic energy was obtained by the biofilm, even without dissolved sulfide in the solution to the anode compartment. Therefore, it is likely that the sulfate was formed by bacteria in the biofilm (e.g. *Desulfurivibrio*, which was the dominant species in the biofilm). Furthermore, at the first days of each

experiment, while no biofilm was present yet, the selectivity for sulfur was much higher (see [Figs. 2 and 3](#)). Therefore it is hypothesized that the planktonic bacteria oxidize sulfide to sulfur and that the biofilm oxidize sulfur to sulfate. Hence, it remains a challenge to be able to control the product formation towards sulfur (without dissolved sulfide in solution). Preventing the formation of a biofilm might be an important step to obtain a higher selectivity for sulfur formation.

We have demonstrated that bacteria can take up sulfide in the sulfide uptake reactor and subsequently discharge electrons to the anode of an electrochemical cell without dissolved sulfide present in the electrochemical cell. This reduces the risk of electrode passivation resulting from sulfur deposition on the anode via electrochemical oxidation. This electrode passivation is problematic in (bio)electrochemical systems for direct sulfide removal. We have used XRD to determine the presence of elemental sulfur on the electrode and no elemental sulfur was detected. Future research should focus on the sulfur deposition to confirm that the electron shuttling approach prevents electrodeposition of elemental sulfur.

Another advantage is that, due to the application of haloalkaliphilic bacteria, the system can be operated at high salt concentrations (1 M Na⁺) and alkaline conditions (pH 8–9). This reduces ohmic resistances, resulting in a higher energy efficiency of the bioelectrochemical system compared to systems operated at neutrophilic conditions and low salt concentrations. Compared to conventional biodesulfurization processes, no energy is required for e.g. aeration of the bioreactor and energy from the oxidation of sulfide is recovered. This will improve the energy efficiency of biological gas desulfurization under haloalkaline conditions.

CRedit authorship contribution statement

Rieks de Rink planned and performed experiments, analyzed the results and wrote the manuscript. **Micaela Lavender** and **Dandan Liu** supported experimental work and data analysis. **Jan Klok**, **Annemiek**

ter Heijne and Cees Buisman supported study organization and data analysis and revised the manuscript. Dimitry Sorokin supported data analysis and revised the manuscript. All authors read and approved the manuscript.

Declaration of Competing Interest

The authors declare that they have no known competing financial interests or personal relationships that could have appeared to influence the work reported in this paper.

Acknowledgements

This research was financed by Paqell B.V., the Netherlands We thank Ilse Gerrits for help with the XRD analysis and Marion Meima and Sven Warris for help with the DNA extractions and bioinformatics.

Appendix A. Supporting information

Supplementary data associated with this article can be found in the online version at doi:10.1016/j.jhazmat.2021.127358.

References

- Ateya, B., AlKharafi, F., Al-Azab, A., 2003. Electrodeposition of sulfur from sulfide contaminated brines. *Electrochem. Solid State Lett.* 6 (9), C137–C140.
- Buisman, C., Post, R., Ijspeert, P., Geraats, G., Lettinga, G., 1989. Biotechnological process for sulphide removal with sulphur reclamation. *Acta Biotechnol.* 9 (3), 255–267.
- Burns, D.A., Aherne, J., Gay, D.A., Lehmann, C., 2016. Acid rain and its environmental effects: recent scientific advances. *Atmos. Environ.* 146, 1–4.
- de Rink, R., Klok, J.B., van Heeringen, G.J., Keesman, K.J., Janssen, A.J., ter Heijne, A., Buisman, C.J., 2020. Biologically enhanced hydrogen sulfide absorption from sour gas under haloalkaline conditions. *J. Hazard. Mater.* 383, 121104.
- De Rink, R., Klok, J.B., Van Heeringen, G.J., Sorokin, D.Y., Ter Heijne, A., Zeijlmaaker, R., Mos, Y.M., De Wilde, V., Keesman, K.J., Buisman, C.J., 2019. Increasing the selectivity for sulfur formation in biological gas desulfurization. *Environ. Sci. Technol.* 53 (8), 4519–4527.
- Dutta, P.K., Rabaey, K., Yuan, Z., Keller, J., 2008. Spontaneous electrochemical removal of aqueous sulfide. *Water Res.* 42 (20), 4965–4975.
- Hoef, S.E., Blum, J.S., Stolz, J.F., Tabita, F.R., Witte, B., King, G.M., Santini, J.M., Oremland, R.S., 2007. *Alkalilimnicola ehrlichii* sp. nov., a novel, arsenite-oxidizing haloalkaliphilic gammaproteobacterium capable of chemoautotrophic or heterotrophic growth with nitrate or oxygen as the electron acceptor. *Int. J. Syst. Evolut. Microbiol.* 57 (3), 504–512.
- Janssen, A., Sleyster, R., Van der Kaa, C., Jochemsen, A., Bontsema, J., Lettinga, G., 1995. Biological sulphide oxidation in a fed-batch reactor. *Biotechnol. Bioeng.* 47 (3), 327–333.
- Janssen, A.J., Lens, P.N., Stams, A.J., Plugge, C.M., Sorokin, D.Y., Muyzer, G., Dijkman, H., Van Zessen, E., Luimes, P., Buisman, C.J., 2009. Application of bacteria involved in the biological sulfur cycle for paper mill effluent purification. *Sci. Total Environ.* 407 (4), 1333–1343.
- Kiragosyan, K., Roman, P., Keesman, K.J., Janssen, A.J., Klok, J.B., 2020. Stoichiometry-driven heuristic feedforward control for oxygen supply in a biological gas desulfurization process. *J. Process Control* 94, 36–45.
- Klok, J.B., van den Bosch, P.L., Buisman, C.J., Stams, A.J., Keesman, K.J., Janssen, A.J., 2012. Pathways of sulfide oxidation by haloalkaliphilic bacteria in limited-oxygen gas lift bioreactors. *Environ. Sci. Technol.* 46 (14), 7581–7586.
- Klok, J.B., van Heeringen, G., De Rink, R., Wijnbelt, H., 2017. Introducing the Next Generation of the THIOPAQ O&G Process for Biotechnological Gasdesulfurization: THIOPAQ-SQ.
- Krayzelova, L., Bartacek, J., Diaz, I., Jeison, D., Volcke, E.I., Jenicek, P., 2015. Microaeration for hydrogen sulfide removal during anaerobic treatment: a review. *Rev. Environ. Sci. Bio Technol.* 14 (4), 703–725.
- Lichstein, H.C., Soule, M.H., 1944. Studies of the effect of sodium azide on microbial growth and respiration: I. The action of sodium azide on microbial growth. *J. Bacteriol.* 47 (3), 221.
- Müller, H., Bosch, J., Griebler, C., Damgaard, L.R., Nielsen, L.P., Lueders, T., Meckenstock, R.U., 2016. Long-distance electron transfer by cable bacteria in aquifer sediments. *ISME J.* 10 (8), 2010–2019.
- Muyzer, G., Sorokin, D.Y., Mavromatis, K., Lapidus, A., Clum, A., Ivanova, N., Pati, A., d'Haeseleer, P., Woyke, T., Kyrpides, N.C., 2011. Complete genome sequence of “*Thioalkalivibrio sulfidophilus*” HL-EbGr7. *Stand. Genom. Sci.* 4 (1), 23–35.
- Ni, G., Harnawan, P., Seidel, L., Ter Heijne, A., Sleutels, T., Buisman, C.J., Dopson, M., 2019. Haloalkaliphilic microorganisms assist sulfide removal in a microbial electrolysis cell. *J. Hazard. Mater.* 363, 197–204.
- O'Brien, D.J., Birkner, F.B., 1977. Kinetics of oxygenation of reduced sulfur species in aqueous solution. *Environ. Sci. Technol.* 11 (12), 1114–1120.
- Pfennig, N., Lippert, K.D., 1966. Über das vitamin B 12-bedürfnis phototropher Schwefelbakterien. *Arch. für Mikrobiol.* 55 (3), 245–256.
- Poser, A., Lohmayer, R., Vogt, C., Knoeller, K., Planer-Friedrich, B., Sorokin, D., Richnow, H.-H., Finster, K., 2013. Disproportionation of elemental sulfur by haloalkaliphilic bacteria from soda lakes. *Extremophiles* 17 (6), 1003–1012.
- Rabaey, K., Van de Sompel, K., Maignien, L., Boon, N., Aeltermann, P., Clauwaert, P., De Schampelaere, L., Pham, H.T., Vermeulen, J., Verhaege, M., 2006. Microbial fuel cells for sulfide removal. *Environ. Sci. Technol.* 40 (17), 5218–5224.
- Soloz, M., Carafoli, E., Ludwig, B., 1982. The cytochrome c oxidase of *Paracoccus denitrificans* pumps protons in a reconstituted system. *J. Biol. Chem.* 257 (4), 1579–1582.
- Sorokin, D.Y., Merkel, A.Y. 2020. Bergey's Manual of Systematics of Archaea and Bacteria. Whitman, W.B. (ed), John Wiley & Sons.
- Sorokin, D.Y., Muntyan, M.S., Panteleeva, A.N., Muyzer, G., 2012. *Thioalkalivibrio sulfidophilus* sp. nov., a haloalkaliphilic, sulfur-oxidizing gammaproteobacterium from alkaline habitats. *Int. J. Syst. Evolut. Microbiol.* 62 (8), 1884–1889.
- Sorokin, D.Y., Tourova, T., Mußmann, M., Muyzer, G., 2008a. *Dethiobacter alkaliphilus* gen. nov. sp. nov., and *Desulfurivibrio alkaliphilus* gen. nov. sp. nov.: two novel representatives of reductive sulfur cycle from soda lakes. *Extremophiles* 12 (3), 431–439.
- Sorokin, D.Y., Van Den Bosch, P., Abbas, B., Janssen, A., Muyzer, G., 2008b. Microbiological analysis of the population of extremely haloalkaliphilic sulfur-oxidizing bacteria dominating in lab-scale sulfide-removing bioreactors. *Appl. Microbiol. Biotechnol.* 80 (6), 965–975.
- Sorokin, D.Y., Zhilina, T.N., Lysenko, A.M., Tourova, T.P., Spiridonova, E.M., 2006. Metabolic versatility of haloalkaliphilic bacteria from soda lakes belonging to the *Alkalispirillum-Alkalilimnicola* group. *Extremophiles* 10 (3), 213–220.
- Sun, M., Mu, Z.-X., Chen, Y.-P., Sheng, G.-P., Liu, X.-W., Chen, Y.-Z., Zhao, Y., Wang, H.-L., Yu, H.-Q., Wei, L., 2009. Microbe-assisted sulfide oxidation in the anode of a microbial fuel cell. *Environ. Sci. Technol.* 43 (9), 3372–3377.
- ter Heijne, A., de Rink, R., Liu, D., Klok, J.B., Buisman, C.J., 2018. Bacteria as an electron shuttle for sulfide oxidation. *Environ. Sci. Technol. Lett.* 5 (8), 495–499.
- Thorup, C., Schramm, A., Findlay, A.J., Finster, K.W., Schreiber, L., 2017. Disguised as a sulfate reducer: growth of the deltaproteobacterium *Desulfurivibrio alkaliphilus* by sulfide oxidation with nitrate. *MBio* 8, 4.
- Vaioipoulou, E., Provijn, T., PrévotEAU, A., Pikaar, I., Rabaey, K., 2016. Electrochemical sulfide removal and caustic recovery from spent caustic streams. *Water Res.* 92, 38–43.
- Van den Bosch, P.L., Sorokin, D.Y., Buisman, C.J., Janssen, A.J., 2008. The effect of pH on thiosulfate formation in a biotechnological process for the removal of hydrogen sulfide from gas streams. *Environ. Sci. Technol.* 42 (7), 2637–2642.
- Van Den Bosch, P.L., van Beusekom, O.C., Buisman, C.J., Janssen, A.J., 2007. Sulfide oxidation at haloalkaline conditions in a fed-batch bioreactor. *Biotechnol. Bioeng.* 97 (5), 1053–1063.
- Van Zessen, E., Janssen, A., De Keizer, A., Heijne, B., Peace, J., Abry, R., 2004. Application of THIOPAQTM biosulphur in agriculture, 57–68.
- Walker, D.J., Adhikari, R.Y., Holmes, D.E., Ward, J.E., Woodard, T.L., Nevin, K.P., Lovley, D.R., 2018. Electrically conductive pili from pilin genes of phylogenetically diverse microorganisms. *ISME J.* 12 (1), 48–58.
- Wenhui, L., Bo, G., Zhongning, Z., Jianyong, Z., Dianwei, Z., Ming, F., Xiaodong, F., Lunju, Z., Quanyou, L., 2010. H₂S formation and enrichment mechanisms in medium to large scale natural gas fields (reservoirs) in the Sichuan Basin. *Petroleum Exploration and Development* 37(5), 513–522.
- Zhang, B., Zhao, H., Shi, C., Zhou, S., Ni, J., 2009. Simultaneous removal of sulfide and organics with vanadium (V) reduction in microbial fuel cells. *J. Chem. Technol. Biotechnol.* 84 (12), 1780–1786.

Supplementary material

Continuous electron shuttling by sulfide oxidizing bacteria as a novel strategy to produce electric current

Rieks de Rink^{1,2}, Micaela B. Lavender¹, Dandan Liu², Johannes B.M. Klok^{1,2,3}, Dimitry Y. Sorokin^{4,5}, Annemiek ter Heijne*¹, Cees J.N. Buisman^{1,3}

1. Environmental Technology, Wageningen University, P.O. Box 17, Wageningen, the Netherlands
2. Paqell B.V., Reactorweg 301, 3542 AD Utrecht, the Netherlands
3. Wetsus, European Centre of Excellence for Sustainable Water Technology, Oostergoweg 9, Leeuwarden, the Netherlands
4. Winogradsky Institute of Microbiology, Research Centre of Biotechnology RAS, Leninskii Prospect, 33/2, 119071 Moscow, Russia
5. Department of Biotechnology, Delft University of Technology, Van der Maasweg 9, 2629HZ Delft, the Netherlands

* Corresponding author. Environmental Technology, Wageningen University, P.O. Box 17, 6700 AA Wageningen, the Netherlands. Visiting address: Bornse Weilanden 9, 6708 WG Wageningen, Building Axis z, building nr. 118.

Email address: Annemiek.terheijne@wur.nl

A: Overview of liquid flow rates and HRT's	2
B: NGS details	3
C: XRD measurements	7
D: Sulfide concentrations	9

1

2 **A: Overview of liquid flow rates and HRT's**

3

4 An overview of the applied liquid flow rates, liquid volumes in different parts of the system and the
5 HRT's in the different experiments, is provided in Table A.1

6

7 **Table A.1:** overview of the applied liquid flow rates, liquid volumes in different parts of the system and
8 the HRT's in the different experiments

	Exp 1	Exp 2	Exp 3
Recirculation flow rate (L h ⁻¹)	0.6	0.42	0.42
Influent flow rate (L h ⁻¹)	0.23 · 10 ⁻³	0.41 · 10 ⁻³	0.23 · 10 ⁻³
Volume entire system (incl tubing) (L)	0.5	0.5	0.5
Volume sulfide uptake reactor (L)	0.4	0.4	0.4
Volume anode side of the electrochemical cell (L) *	0.016	0.016	0.016
HRT entire system (h)	2174	1220	1274
HRT sulfide uptake reactor (h)	0.67	0.95	0.95
HRT electrochemical cell (h)	0.03	0.04	0.04

9

10 * The liquid volume of the anode side of the electrochemical cell has been calculated according to:

11 Liquid volume (L) = total volume (L) · bed porosity (%)

12 The bed porosity was approximately 48% (calculated as described by: Pushnov, A. S., Calculation of
13 average bed porosity. Chemical and Petroleum Engineering **2006**, 42 (1), 14-17.)

14

15 **B: NGS details**

16

17 **Materials and methods**

18

19 Samples for microbial community analysis were taken from the liquid and the graphite granules at the
20 end of each run. Also a sample of the inoculum (planktonic biomass) was analyzed. For the analysis of
21 planktonic biomass, 2 mL sample was centrifuged for 10 minutes at 14000 g. The biomass pellets and
22 graphite granules were preserved by snap-freezing in liquid nitrogen and stored at -80°C. DNA was
23 extracted using the Powersoil DNA isolation kit (Qiagen) according to the manufacturer's instructions.
24 Subsequently, PCR was used to amplify the V3 and V4 region of the 16S rRNA gene, using primers as
25 described by (Takahashi, Tomita et al. 2014). These primers are targeting both the bacterial and the
26 archaeal 16S rRNA gene. The DNA was sequenced using the Illumina platform and MiSeq sequencer. The
27 paired-end MiSeq reads were merged based on the overlap between the two reads. Only merged
28 sequences were used in subsequent analyses and the non-overlapping pairs were discarded. The 16S-
29 based metagenomics analyses were performed using QIIME (Caporaso, Kuczynski et al. 2010) version
30 1.9.1. After primer sequences were removed from the merged sequence reads, these were placed in a
31 single fasta file using the add_qiime_labels.py script with the options 'cutadapt -m 100 -u 17 -u -21'.
32 OTU picking was performed with the script pick_open_reference_otus.py using the SILVA version 128
33 (Quast, Pruesse et al. 2012) 16S reference database and uclust (Edgar 2010). The RDP classifier (version
34 2.2) (Wang, Garrity et al. 2007) was trained with the same SILVA reference database and subsequently
35 used to classify the OTUs.

36

37 **References**

38

39 Takahashi, S.; Tomita, J.; Nishioka, K.; Hisada, T.; Nishijima, M., Development of a prokaryotic universal
40 primer for simultaneous analysis of Bacteria and Archaea using next-generation sequencing. *PloS one*
41 **2014**, *9* (8).
42 Caporaso, J. G.; Kuczynski, J.; Stombaugh, J.; Bittinger, K.; Bushman, F. D.; Costello, E. K.; Fierer, N.;
43 Pena, A. G.; Goodrich, J. K.; Gordon, J. I., QIIME allows analysis of high-throughput community
44 sequencing data. *Nature methods* **2010**, *7* (5), 335.
45 Quast, C.; Pruesse, E.; Yilmaz, P.; Gerken, J.; Schweer, T.; Yarza, P.; Peplies, J.; Glöckner, F. O., The
46 SILVA ribosomal RNA gene database project: improved data processing and web-based tools. *Nucleic*
47 *Acids Research* **2012**, *41* (D1), D590-D596.
48 Edgar, R. C., Search and clustering orders of magnitude faster than BLAST. *Bioinformatics* **2010**, *26* (19),
49 2460-2461.
50 Wang, Q.; Garrity, G. M.; Tiedje, J. M.; Cole, J. R., Naive Bayesian classifier for rapid assignment of rRNA
51 sequences into the new bacterial taxonomy. *Applied and environmental microbiology* **2007**, *73* (16),
52 5261-5267.

53 **Results**

54

55 **Table A.2:** Overview of the bacterial species in the solution (planktonic biomass) and attached to the electrode (biofilm) as analyzed via 16S rRNA
 56 amplicon sequencing.

	Relative abundances					Key physiology	Occurrence (Alkaline habitat)
	Inoculum	End of exp 1 (planktonic)	End of exp 1 (biofilm)	End of exp 2 (planktonic)	End of exp 1 (biofilm)		
Sulfide oxidizing bacteria (SOB)							
<i>Proteobacteria / Gammaproteobacteria / Chromatiales / Ectothiorhodospiraceae / Alkalilimnicola</i>	18.48%	18.58%	4.02%	6.36%	1.94%	facultatively autotrophic and facultatively denitrifying SOB	Soda lakes and biodesulfurization plants
<i>Proteobacteria / Gammaproteobacteria / Chromatiales / Ectothiorhodospiraceae / Thioalkalispira</i>	0.22%	1.21%	0.12%	3.34%	0.23%	microaerophilic lithoautotrophic SOB	Soda lakes
<i>Proteobacteria / Gammaproteobacteria / Chromatiales / Ectothiorhodospiraceae / Thioalkalivibrio *</i>	31.88%	2.54%	0.75%	16.40%	9.93%	Lithoautotrophic SOB	Soda lakes and Thiopaq reactors
<i>Proteobacteria / Gammaproteobacteria / Thiotrichales / Piscirickettsiaceae / Thioalkalimicrobium</i>	3.00%	2.90%	0.34%	0.73%	0.99%	Lithoautotrophic SOB	Soda lakes and Thiopaq reactors
<i>Proteobacteria / Gammaproteobacteria / Oceanospirillales / Halomonadaceae Halomonas</i>	1.27%	0.17%	0.23%	0.81%	1.63%	heterotrophic SOB forming tetrathionate	soda lakes and Thiopaq reactors
<i>Proteobacteria / Alphaproteobacteria / Rhodobacterales / Rhodobacteraceae / Other</i>	28.75%	2.59%	0.42%	9.38%	2.43%	Might be photoheterotrophic anaerobic SOB	Might be in soda lakes
<i>Proteobacteria / Epsilonproteobacteria / Campylobacteriales / Campylobacteraceae / Arcobacter</i>	0.06%	3.08%	0.08%	14.30%	0.86%	Microaerophilic sulfide oxidation	Marine
Anaerobic sulfur bacteria							
<i>Proteobacteria / Deltaproteobacteria / Desulfobacterales / Desulfobulbaceae / Desulfurivibrio **</i>	1.28%	21.59%	36.97%	11.11%	43.31%	Elemental sulfur disproportionation or sulfur reduction with H ₂	Biodesulfurization plants
<i>Chrysiogenetes / Chrysiogenetes /</i>	0.35%	1.10%	6.03%	0.35%	1.38%	Sulfur reduction;	Soda lakes

<i>Chrysiogenales / Chrysiogenaceae / Desulfurispirillum</i>						dissimilatory ammonification	
Fermentative bacteria							
<i>Tenericutes / Mollicutes / Acholeplasmatales / Acholeplasmataceae / Acholeplasma</i>	0.58%	6.10%	0.67%	3.44%	1.99%	Fermentative	Found in soda lake metagenomes
<i>Firmicutes / Clostridia / Clostridiales / Clostridiaceae 2 / Anoxynatronum</i>	0.83%	0.92%	1.30%	0.28%	2.73%	Fermentative	Soda lakes
<i>Firmicutes / Clostridia; / Clostridiales / Clostridiaceae 2 / Tindallia</i>	0.40%	0.14%	1.89%	0.16%	1.51%	Acetogenic, can use H ₂ and reduce thiosulfate	Soda lakes
<i>Cloacimonetes / MSBL8 / uncultured bacterium / uncultured bacterium / uncultured bacterium</i>	0.00%	2.12%	2.84%	0.10%	0.40%	Fermentative	Found in soda lake metagenomes
<i>Tenericutes / Mollicutes / NB1-n / Other / Other</i>	0.43%	1.71%	0.79%	0.97%	0.42%	fermentative	found in soda lake metagenomes
<i>Firmicutes / Clostridia / Clostridiales / Clostridiaceae 1 / uncultured</i>	0.11%	0.72%	3.25%	0.05%	0.26%	?	?
<i>Firmicutes / Clostridia / ML635J-38 / uncultured bacterium / uncultured bacterium</i>	0.14%	0.07%	1.12%	0.07%	0.83%		
<i>Firmicutes / Clostridia / Clostridiales / Syntrophomonadaceae / uncultured</i>	0.02%	0.68%	0.39%	0.41%	1.04%	syntrophic oxidation of fatty acids at anaerobic conditions	there are isolates from soda lakes
<i>Firmicutes / Erysipelotrichia / Erysipelotrichales / Erysipelotrichaceae / Erysipelothrix</i>	0.77%	0.43%	0.69%	0.82%	1.08%		
Hydrolytic bacteria							
<i>Bacteroidetes / Sphingobacteriia / Sphingobacteriales / Lentimicrobiaceae / uncultured bacterium</i>	0.24%	15.69%	3.69%	16.13%	8.02%	Polysaccharidolytic	Soda lakes
<i>Bacteroidetes; / Bacteroidia / Bacteroidales / Marinilabiaceae / Natronoflexus</i>	0.00%	0.03%	7.31%	0.01%	0.45%	sugar fermentation	Soda lakes
<i>Bacteroidetes / Bacteroidia / Bacteroidales / ML635J-40 aquatic group / uncultured bacterium</i>	0.01%	0.65%	2.18%	0.95%	0.83%		soda lakes
<i>Bacteroidetes / Bacteroidia /</i>	0.00%	0.08%	2.08%	0.01%	1.24%		

<i>Bacteroidales / Marinilabiaceae; Ambiguous_taxa</i>							
<i>Bacteroidetes / Bacteroidia / Bacteroidales / Marinilabiaceae / Alkaliflexus</i>	0.00%	0.01%	1.20%	0.00%	0.10%	sugar fermentation	soda lake
<i>Bacteroidetes / Bacteroidia / Bacteroidales / Rikenellaceae / Blvii28 wastewater-sludge group</i>	0.03%	0.08%	1.63%	0.33%	1.37%		
<i>Bacteroidetes / Bacteroidia / Bacteroidia Incertae Sedis / Draconibacteriaceae / uncultured</i>	0.08%	0.14%	0.41%	0.35%	1.88%	sugar fermentation	

57

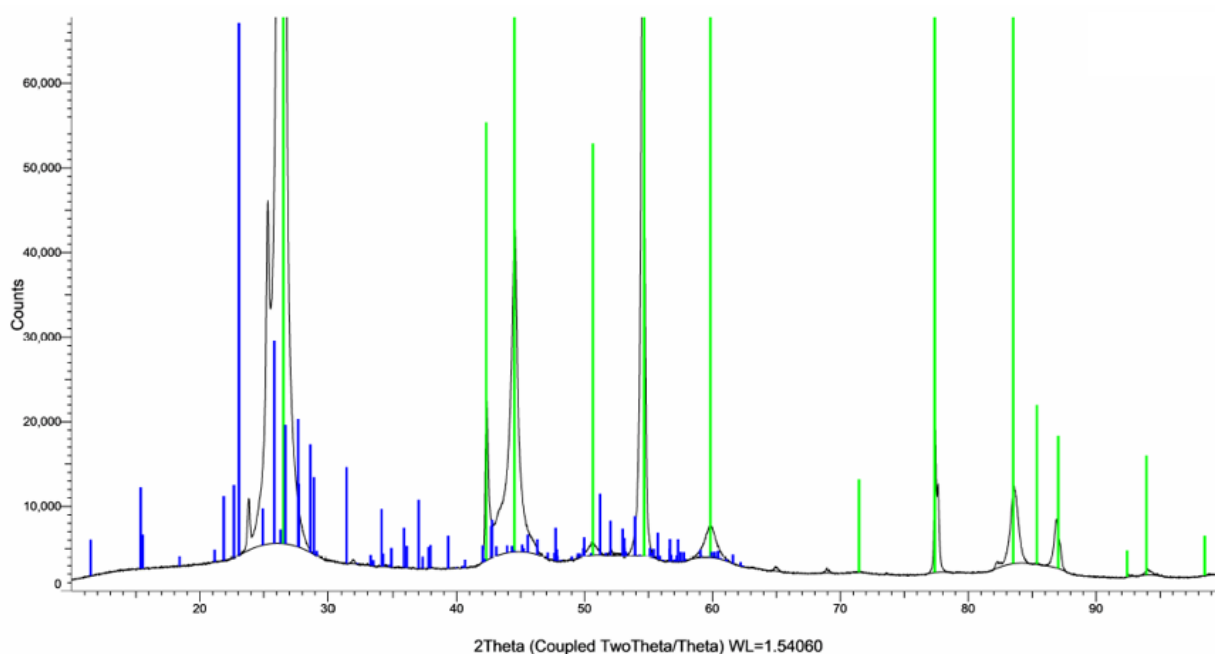
58 * Until recently, *Thioalkalivibrio* was classified as a member of the family *Ectothiorhodospiraceae* (*Gammaproteobacteria*). It has been suggested
59 to reclassify the genus *Thioalkalivibrio* into its own family *Thioalkalivibrionaceae* within the order *Ectothiorhodospirales* on the basis of the
60 emerging phylogenetic taxonomy (<https://gtdb.ecogenomic.org>).

61

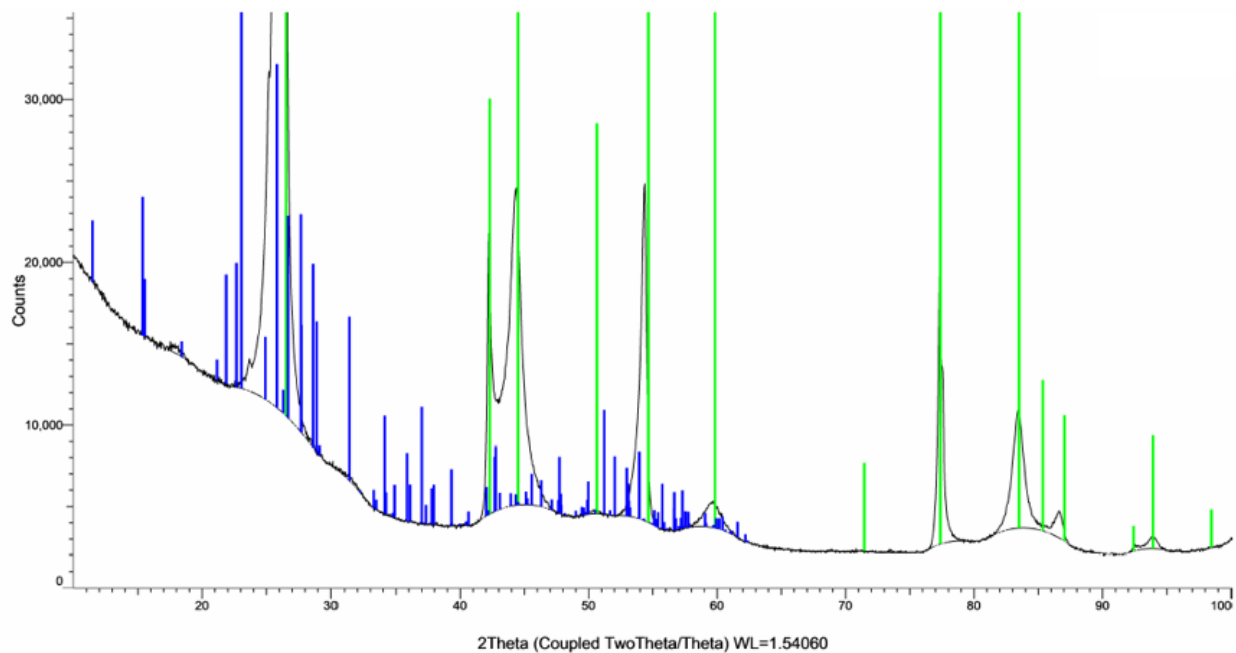
62 ** The higher taxonomy recently has been changed to *Desulfobulbia*>*Desulfobulbales*:*Desulfurivibrionaceae*.

63 **C: XRD measurements**

64 At the end of each experiment, the presence of elemental sulfur on the working electrode (i.e. the
65 graphite granules and the graphite plate of the anolyte side of the electrochemical cell) was verified
66 with XRD analysis. The measurements were done with a Bruker D8 Advance powder diffractometer with
67 Lynxeye detector in Bragg Brentano geometry. Figures C.1 and C.2 show the XRD spectra of the granules
68 and plate at the end of experiment 2. The XRD spectra corresponds to graphite (the electrode material),
69 but doesn't indicate presence of S₈ sulfur. Spectra after experiment 1 and after the abiotic experiment
70 indicate the same.



71
72 **Figure C.1:** XRD spectrum of graphite granules at end of experiment 2. The measurement was done from
73 10 to 100 deg 2 theta, with steps of 0,02 deg, time/step 3s. The measured spectrum is shown by the
74 black line. XRD spectrum of graphite is indicated in green; XRD spectrum of S₈ sulfur is indicated in blue.



75

76 **Figure C.2:** XRD spectrum of the graphite plate at the end of experiment 2. The measurement was done
 77 from 10 to 100 deg 2 theta, with steps of 0,05 deg, time/step 1s and xyz-sample stage. The measured
 78 spectrum is shown by the black line. XRD spectrum of graphite is indicated in green; XRD spectrum of S₈
 79 sulfur is indicated in blue.

80 **D: Sulfide concentrations**

81 The sulfide uptake was determined by measuring sulfide in the in the sulfide uptake reactor. In
82 experiment 1, lead acetate paper was used. This indicates the presence or absence of sulfide. In
83 experiment 2, the sulfide concentration was also measured using Hach Lange kit LCK635. The results are
84 shown in figure D.1.

85

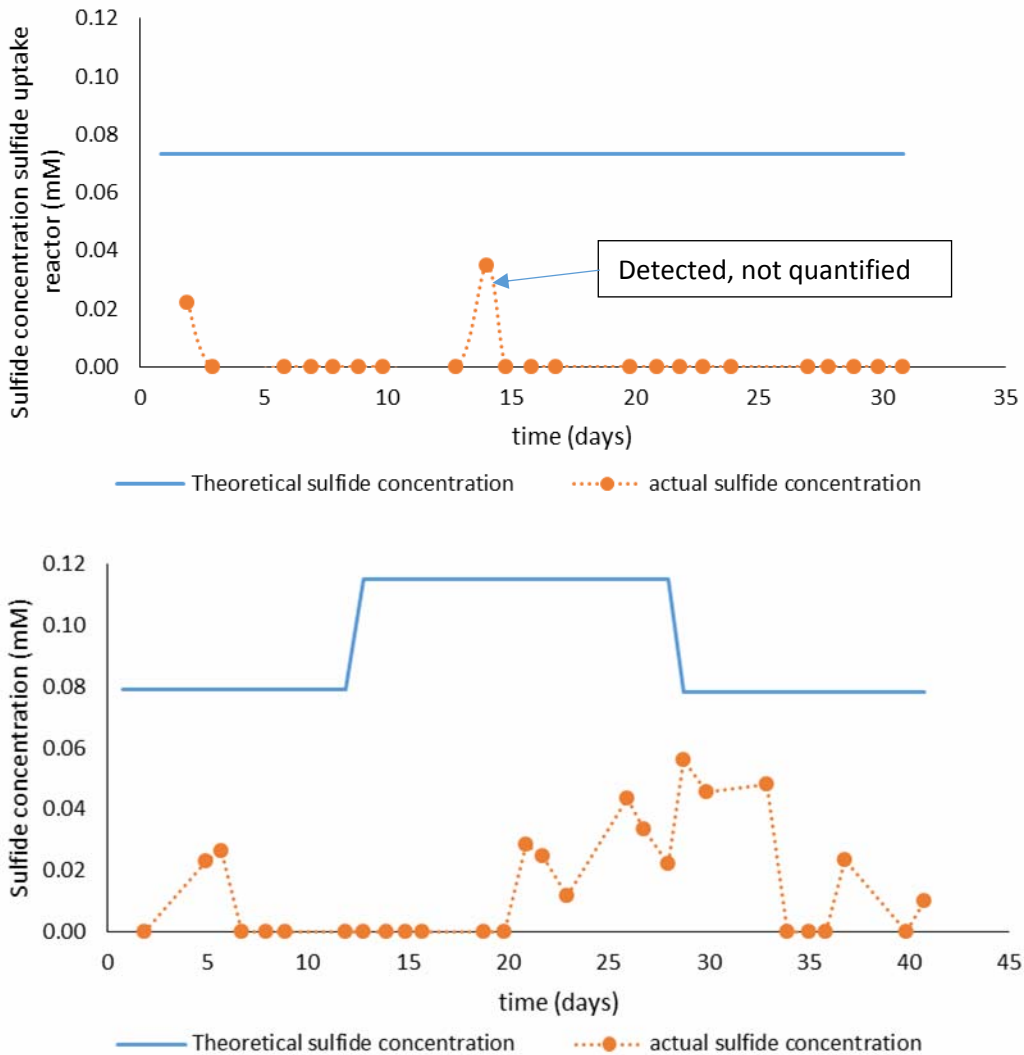


Figure D.1: The actual and measured sulfide concentrations in experiments 1 (top) and 2 (bottom). The blue line indicates the theoretical sulfide concentration in the sulfide uptake reactor, which is set by the sulfide dosing rate and the recirculation flow rate. The orange dots indicate the measured sulfide concentration in the sulfide uptake reactor.